Journal of Control, Automation and Electrical Systems (2021) 32:153–164
https://doi.org/10.1007/s40313-020-00660-2

Robust Controller of Buck Converter Feeding Constant Power Load

Mahmoud S. Ali[1] · M. Soliman[2] · Ahmed M. Hussein[2] · Said A. F. Hawash[1]

Received: 24 April 2020 / Revised: 12 September 2020 / Accepted: 27 October 2020 / Published online: 17 November 2020

Abstract
In this paper, we propose a robust PID controller based on Kharitonov theorem to overcome stability issues in DC power systems. These issues are caused by increasing number of constant power loads (CPLs), uncertainty in the input voltage and disturbances which affect the system performance. We designed this controller for achieving the desired tracking performance and closed-loop stability of DC buck converter that feeds constant impedance load and CPL. The drawback of small signal stability methods was handled as the system is linearized around all the possible operating points which is the main contribution of this paper. To assure stability over the operating range, Hermit Biehler theorem is used to find the stabilization sets of the PID controller. Stability analysis reveals that the proposed method is robust for uncertainties. The simulation results show promising performance of the proposed algorithm of the PID controller.

Keywords DC microgrid · Kharitonov · Hermite Biehler · Constant power load

List of Symbols

L	Inductance
r_L	Inductor resistance
i_L	Inductor current
C	Capacitance
R	Resistance of the resistive load
v_o	Output voltage
v_s	Supply voltage
$u \in (0, 1)$	Control signal
P	Power of the CPL
V_{ref}	Desired reference voltage
V_s, U, V_o and I_L	Average values of v_s, u, v_o. and i_L, respectively
$\tilde{v}_s$, $\tilde{u}$, $\tilde{v}_o$ and $\tilde{i}_L$	Small signal disturbances of v_s, u, v_o. and i_L, respectively
$\delta(s)$, $\delta(j\omega)$	Characteristic polynomial in frequency domain
s	Normalized characteristic polynomial
$\sigma_i(\delta)$	Imaginary signature of the characteristic polynomial
$\delta_e(s^2)$, $\delta_o(s^2)$	Even and odd components of $\delta(s)$
$N(s)$, $D(s)$	Nominator and denominator of plant transfer function
$p(\omega)$, $q(\omega)$	Real and imaginary components of $\delta(j\omega)$
$p_f(\omega)$, $q_f(\omega)$	Real and imaginary components of $\delta_f(j\omega)$
$\theta(\omega)$	Phase angle of $\delta_f(j\omega)$
$\Delta_0^\infty\theta$	Net change in the phase angle $\theta(\omega)$
$l(\delta)$, $r(\delta)$	Number of roots of $\delta_f(j\omega)$ in left and right half plane, respectively
I	String contains all possible signs of $p_f(\omega)$
$\gamma(I)$	Imaginary signature related to string I
K_p, K_i, K_d	Proportional, integral and derivative gains of PID controller
$n_c(s)$, $d_c(s)$	Nominator and denominator of PID Transfer function
$\underline{b_0}$, $\overline{b_0}$, $\underline{a_1}$, $\overline{a_1}$, $\underline{a_0}$, $\overline{a_0}$	Lower and upper bounds of b and a, respectively

✉ Mahmoud S. Ali
mahmmod.shaban@yahoo.com

M. Soliman
msoliman1512@gmail.com

Ahmed M. Hussein
ahmed.hussein@feng.bu.edu.eg

Said A. F. Hawash
saidhawash64@yahoo.com

[1] Department of Control Engineering, Mechanical and Electrical Research Institute, National Water Research Center, El-Kanater El-Khayrya, Cairo, Egypt

[2] Electrical Engineering Department, Faculty of Engineering at Shoubra, Benha University, Cairo, Egypt

$K(s)$	Kharitonov polynomial
$NS(s)$	Kharitonov segments of $N(s)$

1 Introduction

With everyday advancement in semiconductor technology, power electronic converters (PECs) are becoming more efficient, reliable, cheaper, and smaller in size. With the help of PECs, distributed DC power systems are now becoming more beneficial than AC distribution systems in terms of efficiency, reliability, cost, size, etc.

Renewable energy resources (RERs), such as wind and solar energy, attract more attention nowadays to reduce Co2 emissions and decrease depending on fossil fuel. The importance of RER arises in isolated areas such as desert which is difficult to be connected to the power grid. However, depending on RER is more challenging due to different types of loads and the intermittent nature of RER. A combination of different sources and loads is called microgrid (MG) which differs from DC to AC or a combination of them. A DC MG is preferred over AC MG due to higher reliability, uninterruptible power supply, no reactive power-reduction in losses, no harmonics, no need for synchronization, no frequency challenges, higher efficiency, and direct connection with DC bus for DC loads such as LED, TV, laptop, and washing machines (Lu et al. 2016).

Stability is a serious issue that appeared in DC microgrid which may cause the whole system to collapse. The main cause of stability issue in DC microgrid is the constant power loads (CPLs) which is reviewed in the next sections.

1.1 Literature Review

The stability problem which caused by CPLs is a main issue in the DC MG, where it is difficult to find the actual equilibrium point (Zhang et al. 2018; Lonkar and Ponnaluri 2015). The typical reason of the instability in DC power system is due to cascaded converters as shown in Fig. 1, where these converters are often referred as the CPLs. In CPL, if the input current increases the input voltage decreases and vice versa to keep power constant. Therefore, CPL introduces a negative impedance characteristic in low frequency range at the input terminal that tends to oscillate with the output impedance of power supply filter (Nahid-Mobarakeh et al. 2016; Dong et al. 2017). Consequently, an impedance mismatch between lightly damped filters, at the source side, and the tightly regulated power converters, at the load side, is occurred.

Constant impedance loads (CILs) generally increase damping, whereas CPLs tend to decrease damping because of the negative incremental impedance is seen by the source. The negative impedance causes moving the system poles to the right-half plane which causes instability for the system.

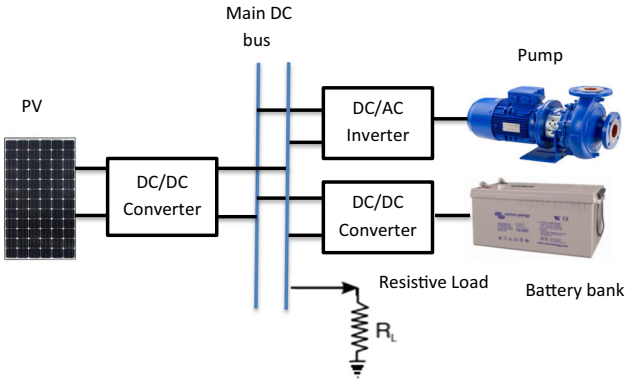

Fig. 1 Distributed DC power system

In practice, speed regulated motor drives and electronic loads may introduce such a destabilizing effect. If the motor speed is controlled to be constant, the torque will be constant with one to one torque-speed characteristic causing the power to be constant. Therefore, these loads act as CPLs (Emadi et al. 2006).

1.1.1 Passive Damping Techniques

The common way to compensate the impedance criteria is to smooth the resonant peak of the input filter by adding physical resistors in series and/or parallel with respective inductors and capacitors or increasing the capacitor value. This approach is commonly considered as a passive stabilization (Dragičević et al. 2016). However, adding physical damping elements introduces dissipative losses to the system and increases cost and size. Therefore, researchers have come up with active damping solutions, where stabilization can be achieved only by modifying the point of load converter or the closed-loop converter.

1.1.2 Active Damping Techniques

Active damping methods can be divided into small- and large-signal strategies (Dragičević et al. 2016). The basic principle in small-signal stabilization methods is using linear feedback laws (Emadi and Ehsani 2000; Rahimi and Emadi 2009).The drawback of the linear feedback stabilization techniques is the fact that they are valid only for analyzing the operating point and operate around that point, but it may not operate perfectly outside its neighborhood. Therefore, it is sometimes preferable to develop advanced control strategy for the drives when the power of the CPL considerably varies (Dragičević et al. 2016). The nonlinear analysis tools are used to obtain valid conditions for global stability realized by linear controllers. In that sense, large signal analysis with phase plane was introduced for buck and boost converters feed CPL (Rivetta and Williamson 2003; Williamson and Rivetta 2004),

where a state feedback control law is divided into three regions which are analyzed based on some constraints to check the stability using phase plane analysis. In Kwasinski and Krein (2007), another method using nonlinear passivity theory, a PD controller can assure the global stability of a DC MG. There is another approach to achieve the large-signal stability, by using the nonlinear controllers. A geometric based on nonlinear method, referred to as the boundary control which is employed to drive the source converter to feed the CPL toward the desired operating point (Onwuchekwa and Kwasinski 2010). This technique tracks the state variables of the source converter in order to select a boundary at which the switching occurs. It provides easy method to make system stable but the selected boundary was linear which reduce its ability to maintain system stable at large CPL variations. A large signal method using T-S Fuzzy approximates the nonlinear DC MG system with linear systems and study the region of attraction around some given equilibrium points (Herrera et al. 2017). A sliding-mode duty-ratio controller for DC/DC buck converters of shipboard power system was proposed in Zhao et al. (2014); however it didn't prove global stability. A linear stability analysis using the Jacobian matrix in order to test the proposed nonlinear sliding mode controller was proposed in Tahim (2011); however stability analysis was calculated based on restricted conditions related to the connected constant impedance load. In Zhang et al. (2018) the system of a polytopic uncertainty set is linearized and the convex optimization problem is solved to find the equilibrium point. However, there is conservativeness in their solution. The Lyapunov function with discontinuous controller is proposed in Perez and Hossain (2017), but there is chattering issues because of the discontinuous sliding mode controller. It doesn't also test the proposed method for different CPLs. Discrete time modeling for multiple CPLs and stabilizer with virtual impedance was proposed in Gavagsaz-Ghoachani et al. (2015). When the parameters such as inductance and capacitance of the converters are equal or close in a certain range, the system will lose stability because of the resonance, a proposed design criteria to control the parallel sources feeding CPL by solving a Jacobian matrix to determine stability range (Dong et al. 2017); however it was operated around linearized equilibrium point. Hysteresis current controller with a proportional-integral (PI) algorithm to regulate the output voltage of the converter was proposed in Rivetta et al. (2006). A proposed nonlinear feedback loop which is called a loop-cancellation technique has been developed in Williamson et al. (2010), where the loop is placed in parallel with the classical voltage feedback path to achieve zero steady-state error and damping at the same time. A nonlinear controller was proposed in Nahid-Mobarakeh et al. (2009) to control a permanent magnet synchronous motor (PMSM)-based voltage source inverter. The large signal analysis proved that it is very helpful to understand the behavior of CPLs. It helps to control the system that has large changes around operating point caused by connection or disconnection of large loads or generators. A unified impedance-based stability criterion method was proposed for grid connected inverters in Ye (2017), where it check stability of global minor loop gain of the parallel inverters. If global minor loop gain meets Nyquist stability criterion, then system is stable. It is very simple method and doesn't need over calculation when the system complexity increases, but it suffers from instability when grid impedance or number of connected inverters have been increased about certain limits. In a cascaded converter system (Ahmadi 2013), any change in downstream converter caused disturbance to the upstream converter but there is a time delay in its feedback loop that degrade system stability so an extra feedback loop was introduced from the downstream to the upstream converter to stabilize it. A distributed adaptive controller was proposed to stabilize DC MG. However, the proposed model reference adaptive control suffers oscillation with high frequency signals (Vu 2016). Hierarchical control was proposed in Srinivasan (2017) which is consisted of primary controller-based passivity approach to insure stability with CPL and integral secondary controller to correct voltage deviations. However, only local asymptotic stability was obtained and it didn't assure global asymptotic stability. Quadratic D-stable fuzzy controller was proposed for DC MG with CPL; it stabilizes the system but suffers from rule expansion with increasing CPLs (Vafamand et al. 2019). Energy buffer power converter for a constant power LED lighting load that presents a controllable input impedance to the electrical source has been proposed in Lindahl et al. (2019). Exact feedback linearization method was also proposed in Hu et al. (2019). All of the previous methods don't assure global asymptotic stability and it didn't consider parameter uncertainties which are the motivation for this work.

1.2 Main Contributions

Based on the above-mentioned results and shortcomings, in this work we propose a simple and robust PID controller based on Kharitonov theorem. This controller is not only able to mitigate the instability issue caused by the CPL nonlinearity but also the uncertainty in system parameters. Moreover, small signal modeling drawbacks have been avoided by designing a robust PID controller for multi-model plant which means that it will be able to operate around different operating points. This can be achieved based on Hermite–Biehler theorem to find the PID stabilization set (Ho et al. 2000). Although Nyquist plot and root locus were used to stabilize the system but these methods are graphical and fail to provide analytical characterization with all stabilizing controller gains. We used the four Kharitonov segments to design a polytope of polynomials to stabilize the multi-model

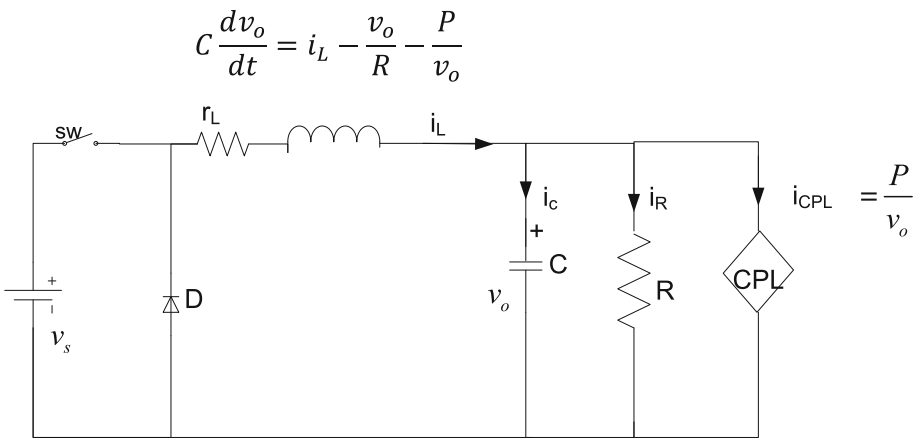

Fig. 2 DC–DC buck converter feed CPL

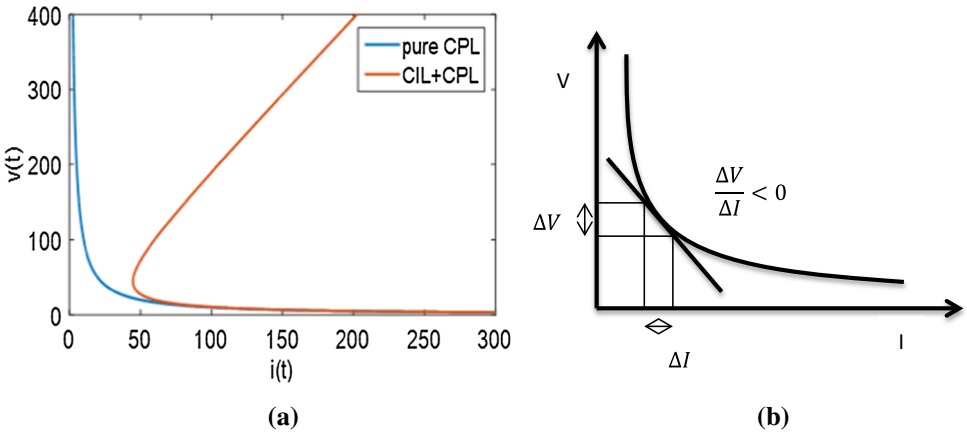

Fig. 3 **a** CPL and CIL characteristic curve, **b** negative resistance of CPL

plant. Our proposed method is compared to the relay method in Grino and Rafiezadeh (2019) to prove its robustness.

2 Problem Formulation

Consider a buck converter delivers a constant power to a CPL as shown in Fig. 2. The dynamic average state-space model of that system is given by (1) (Rivetta and Williamson 2003; Zhao et al. 2014; Grino and Rafiezadeh 2019):

$$\begin{aligned} L\frac{\mathrm{d}i_L}{\mathrm{d}t} &= uv_s - v_o - r_L \cdot i_L \\ C\frac{\mathrm{d}v_o}{\mathrm{d}t} &= i_L - \frac{v_o}{R} - \frac{P}{v_o} \end{aligned} \tag{1}$$

Consider a small disturbance in the state space variables is occurred at v_s and u producing a small disturbance at v_o and i_L as given by (2).

$$\begin{aligned} &v_s = V_s + \tilde{v}_s \text{ and } u = U + u \\ &v_o = V_o + \tilde{v}_o \text{ and } i_L = I_L + \tilde{i}_L \end{aligned} \tag{2}$$

Substituting in (1) gives the system transfer function $G(s)$, which is the ratio of the output voltage to the control signal, as given by (3).

$$G(s) = \frac{\tilde{v}_o}{\tilde{u}} = \frac{\frac{V_s}{LC}}{s^2 + \left(\frac{r_L}{L} + \frac{1}{RC} - \frac{P}{CV_o^2}\right)s + \left(\frac{r_L}{RLC} + \frac{1}{LC} - \frac{r_L P}{LCV_o^2}\right)} \tag{3}$$

The CPL has nonlinear characteristics as shown in Fig. 3. The constant impedance load (CIL) is represented by the linear part, when the load becomes purely CPL it turns to the highly nonlinear curve which resulted in the negative impedance as shown in Fig. 3b.

The characteristic equation obtained from (3) shows that increasing the inductance L or increasing the power P will push poles to the right-half plane (RHP) and make the system unstable. The stability of the system is achieved according to Routh-Hurwitz criterion at the condition explained by (4).

$$\begin{aligned} &\left(\frac{r_L}{L} + \frac{1}{RC} > \frac{P}{CV_o^2}\right) \\ &\left(\frac{r_L}{RLC} + \frac{1}{LC} > \frac{r_L P}{LCV_o^2}\right) \end{aligned} \tag{4}$$

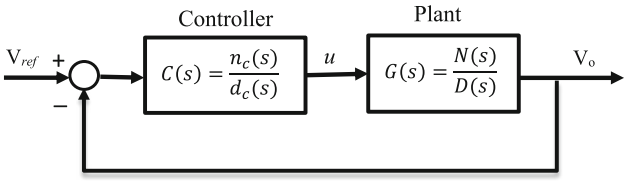

Fig. 4 Block diagram of the closed-loop system

Therefore, the maximum power that the system can deliver before it become unstable is specified by (5):

$$P < \frac{r_L C + (L/R)}{L} V_o^2 \tag{5}$$

Consequently, increasing capacitance or resistive loads may increase stability but there are limits because of the increased cost and size.

3 Proposed Algorithm

To analyze the closed-loop system stability and detect the location of its RHP roots, we propose the following steps:

1. Generate the four Kharitonov rectangles for the uncertain plant.
2. Solve GHB and find the PID stabilizing region.
3. Apply zero exclusion condition to test stability of the selected gains.

Consider the closed-loop system that consists of a controller cascaded with the plant is shown in Fig. 4.

The plant transfer function is assumed to be a rational form given by (6).

$$G(s) = \frac{N(s)}{D(s)} \tag{6}$$

Assume the plant is controlled with a PID controller whose transfer function is given by (7).

$$C(s) = \frac{n_c(s)}{d_c(s)} = \frac{k_d s^2 + k_p s + k_i}{s} \tag{7}$$

The closed-loop transfer function is designated by (8):

$$\frac{Y(s)}{R(s)} = \frac{(k_d s^2 + k_p s + k_i)N(s)}{(k_d s^2 + k_p s + k_i)N(s) + sD(s)} \tag{8}$$

Therefore, the denominator of the closed-loop transfer function is considered as the closed-loop characteristic polynomial $\delta(s, k_p, k_d, k_i)$ of degree n (with real coefficients) and assumed to be given by (9):

$$\delta(s) = \delta_0 + \delta_1 s + \delta_2 s^2 + \delta_3 s^3 + \delta_4 s^4 + \cdots + \delta_n s^n \tag{9}$$

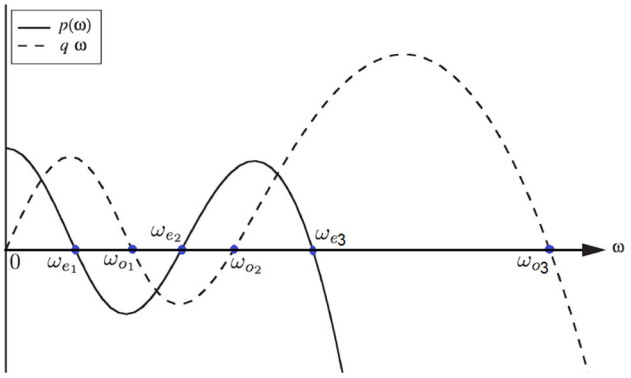

Fig. 5 The interlacing property for Hurwitz polynomials $\delta(s)$

We can divide $\delta(s)$ into two polynomials which are $\delta_e(s^2)$ that include all even powers and $\delta_o(s^2)$ that includes all odd powers of s as given by (10) and (11), respectively

$$\delta(s) = \underbrace{\delta_0 + \delta_2 s^2 + \cdots}_{\delta_e(s^2)} + s\underbrace{(\delta_1 + \delta_3 s^2 \cdots)}_{\delta_o(s^2)} \tag{10}$$

$$\delta(s) = \delta_e\left(s^2\right) + s\delta_o\left(s^2\right) \tag{11}$$

3.1 Hermite–Biehler Theorem

For every frequency $\omega \in \Re$, by replacing each s in the above two equations by $j\omega$, this makes $\delta_e(-\omega^2)$ is a real polynomial and $\delta_o(-\omega^2)$ is an imaginary polynomial. Therefore, the characteristic polynomial $\delta(j\omega)$ will be written as shown by (12):

$$\delta(j\omega) = p(\omega) + jq(\omega) \tag{12}$$

where $p(\omega) = \mathrm{Re}(\delta(j\omega)) = \delta_e\left(-\omega^2\right)$, and $q(\omega) = \mathrm{Im}(\delta(j\omega)) = \omega\delta_o\left(-\omega^2\right)$.

Assuming that $\omega_{e1}, \omega_{e2}, \omega_{e3}, \ldots$ denote the nonnegative real zeros of $\delta_e\left(-\omega^2\right)$. and $\omega_{o1}, \omega_{o2}, \omega_{o3}, \ldots$ denote the nonnegative real zeros of $\delta_o\left(-\omega^2\right)$. arranged in ascending order of magnitude. Then, $\delta(s)$ is Hurwitz stable if and only if all the zeros of $\delta_e\left(s^2\right)$, $\delta_o\left(s^2\right)$ are real and distinct, and their nonnegative real zeros satisfy the following interlacing property is shown in Fig. 5

$$0 < \omega_{e1} < \omega_{o1} < \omega_{e2} < \omega_{o2} < \omega_{e3} < \omega_{o3} \ldots \ldots \tag{13}$$

3.2 Generalized Hermite Biehler Theorem

Assuming $\delta(s)$ be a real polynomial of degree n with k multiple roots at the origin and no imaginary axis roots. This polynomial can be normalized by dividing it by $f(\omega)$, where $f(\omega)$ is given by (14):

$$f(\omega) = \left(1 + \omega^2\right)^{\frac{n}{2}} \tag{14}$$

The normalized polynomial $\delta_f(j\omega)$ can be divided into real and imaginary parts as given by (15):

$$\delta_f(j\omega) = p_f(\omega) + jq_f(\omega) \quad \text{where } p_f(\omega) = \frac{p(\omega)}{(1+\omega^2)^{\frac{n}{2}}} \text{ and } q_f(\omega) = \frac{q(\omega)}{(1+\omega^2)^{\frac{n}{2}}} \tag{15}$$

At any given frequency, ω, the phase angle, θ, of the normalized polynomial, $\delta_f(j\omega)$, is given by (16):

$$\theta(\omega) = \angle\delta_f(j\omega) = \tan^{-1}\left(\frac{q(\omega)}{p(\omega)}\right) \tag{16}$$

Therefore, to select the frequency range to analyze the distribution of the normalized polynomial roots, the change in the phase angle, $\triangle_0^\infty\ \theta$, as ω increases from 0 to ∞ can be given by (17):

$$\triangle_0^\infty\ \theta = \frac{\pi}{2}\left(l\left(\delta_f\right) - r\left(\delta_f\right)\right) \tag{17}$$

Assuming $0 = \omega_0 < \omega_1 < \omega_2 \ldots < \omega_{l-1}$ be the real, nonnegative distinct finite zeros of $q_f(\omega)$ with odd multiplicities. Assuming $\omega_l = \infty$, then the imaginary signature $\sigma_i(\delta)$ is given by (18).

$$\sigma_i(\delta) = \begin{cases} \left\{\text{sgn}[p_f^k(\omega_0)] - 2\text{sgn}[p_f(\omega_1)] + 2\text{sgn}[p_f(\omega_2)] + \cdots + \left(-1\right)^{l-1}\cdot 2\text{sgn}[p_f(\omega_{l-1})]\right. \\ \quad \left. +(-1)^l\text{sgn}[p_f(\omega_l)\right\}.\left(-1\right)^{l-1}\text{sgn}[q(\infty)\Big] & \text{if } n \text{ is even} \\ \left\{\text{sgn}[p_f^k(\omega_0)\Big] - 2\text{sgn}[p_f(\omega_1)\Big] + 2\text{sgn}[p_f(\omega_2)] + \cdots + (-1)^{l-1}\right\} \\ \quad \cdot\left(-1\right)^{l-1}\text{sgn}[q(\infty)\Big] & \text{if } n \text{ is odd} \end{cases} \tag{18}$$

where

$$p_f^k(\omega_0) := \frac{\mathrm{d}^k}{\mathrm{d}\omega^k}\left[p_f(\omega)\right]\Big|_{\omega=\omega_0} \text{ and } \text{sgn}[x] = \begin{cases} -1 & \text{if } x < 0 \\ 0 & \text{if } x = 0 \\ 1 & \text{if } x > 0 \end{cases}$$

The standard signum function, sgn[x], has numbers (− 1, 0 and 1) that called strings and used to capture all possibilities of the sign of $p_f(\omega, k)$ at the real zeros of $q_f(\omega)$.

Each value of $\omega_0, \omega_1, \omega_2, \ldots, \omega_l$, given above, must have a corresponding value of $i_0, i_1, i_2, \ldots, i_l$ where $i_0 \in \{-1, 1\}$ and so do $i_1, i_2, \ldots, i_l$. These values of $i_0, i_1, i_2, \ldots, i_l$ consist the set A of strings where

$$A = \begin{cases} \{i_0, i_1 \ldots i_l\} & \text{if } m+n \text{ is even} \\ \{i_0, i_1 \ldots i_{l-1}\} & \text{if } m+n \text{ is odd} \end{cases}$$

where n and m are the degree of $\delta\left(s, k_\text{p}, k_\text{i}, k_\text{d}\right)$ and $N(s),$, respectively.

For each string $I = \{i_0, i_1, i_2, \ldots, i_l\}$ in A, the imaginary signature $\gamma(I)$ related to string I is calculated as given in (19):

$$\gamma(I) = \begin{cases} \{i_0 - 2i_1 + 2i_2 + \cdots(-1)^{l-1}2i_{l-1} + \left(-1\right)^{l-1}i_l\}\cdot\left(-1\right)^{l-1}\text{sgn}[q(\infty)\Big] & \text{if } n+m \text{is even} \\ \{i_0 - 2i_1 + 2i_2 + \cdots\left(-1\right)^{l-1}2i_{l-1}\}\cdot\left(-1\right)^{l-1}\text{sgn}[q(\infty)\Big] & \text{if } n+m \text{is odd} \end{cases} \tag{19}$$

The appropriate value for $i_0, i_1, i_2, \ldots, i_l$ is selected as 1 or − 1 so that $\gamma(I) = \sigma_i(\delta)$

3.3 Numerical Application

Applying the GHB theorem to the proposed system, and substituting $C = 470$ μF, $L = 100$ μH, $P = 1100$ W,$V_o = 24$v, $V_\text{s} = 48$v, $r_L = 0.05$ Ω and $R = 100$ Ω in the plant transfer function given by (3), it will be as given in (20).

$$G(s) = \frac{N(s)}{D(s)} = \frac{10.2\times10^8}{s^2 - 3764s + 1.9\times10^7} \tag{20}$$

Then, the closed-loop characteristic polynomial, which is the denominator of (20), is given by (21):

$$\delta\left(s, k_p, k_i, k_d\right) = sD(s) + \left(k_i + k_d s^2\right)N(s) + k_p sN(s) \tag{21}$$

Substituting from (20) into (21);

$$\begin{aligned}\delta\left(s, k_p, k_i, k_d\right) = {} & s^3 + \left(10.2\times10^8 k_d - 3764\right)s^2 \\ & + \left(10.2\times10^8 k_p + 1.9\times10^7\right)s \\ & + 10.2\times10^8 k_i\end{aligned} \tag{22}$$

To find k_p, k_i, k_d, we replace $s$by $j\omega$ in (22) then find $p(\omega)$ and $q(\omega)$ as illustrated in (23), (24) and (25).

$$\delta\left(j\omega, k_p, k_i, k_d\right) = 10.2 \times 10^8 k_i + j\omega\left(10.2 \times 10^8 k_p + 1.9 \times 10^7\right) - \omega^2\left(10.2 \times 10^8 k_d - 3764\right) - j\omega^3 \tag{23}$$

$$\delta\left(j\omega, k_p, k_i, k_d\right) = \left\{10.2 \times 10^8 k_i - \omega^2\left(10.2 \times 10^8 k_d - 3764\right)\right\} + j\omega\left\{10.2 \times 10^8 k_p + 1.9 \times 10^7 - \omega^2\right\} \tag{24}$$

$$\delta\left(j\omega, k_p, k_i, k_d\right) = \left[p_1(\omega) + \left(k_i - k_d\omega^2\right) p_2(\omega)\right] + j\left[q_1(\omega) + k_p q_2(\omega)\right] \tag{25}$$

If the above characteristic equation equal zero then the real part and imaginary part equal must be zero too. Therefore, by equating $q(\omega)$ with zero, we get k_p as given by (26):

$$k_p = \frac{-q_1(\omega)}{q_2(\omega)} = \frac{\omega^2 - 1.9 \times 10^7}{10.2 \times 10^8} \tag{26}$$

This resulted in $k_p \in (-0.018, \infty)$.

Performance of PID is beyond the scope of this paper so arbitrarily value for k_p is taken inside the stability range. Therefore, assuming a fixed value for $k_p = 0.1$, inside the stability range, and substituting in $q(\omega)$, then we have the expression given by (27):

$$q(\omega, 0.1) = q_1(\omega) + 0.1 q_2(\omega) = -\omega^3 + 12.1 \times 10^7 \omega \tag{27}$$

So, $q(\omega)$ have two positive real nonnegative finite zeros which are $\omega_0 = 0$ and $\omega_1 = 1.1 \times 10^4$.

According to GHB theorem $\delta\left(j\omega, k_p, k_i, k_d\right)$ is Hurwitz if and only if the imaginary signature $(\sigma_i(\delta))$ given in (18) equals the imaginary signature $\gamma(I)$ given in (19). Therefore, imaginary signature $\sigma_i(\delta)$ is calculated by (28).

$$\sigma_i\left(\delta\left(s, k_p, k_i, k_d\right)\right) = n - (l(N(s)) - r(N(s))) = 3 - (0 - 0) = 3 \tag{28}$$

Since $(1)^{l-1}\text{sgn}[q(\infty)] = (1)^{2-1}(-1) = 1$, and $\gamma(I)$ must equal 3, then:

$$\gamma(I) = (i_0 - 2i_1) \times 1 = 3 \tag{29}$$

The only set of string is $I = \{1, -1\}$ to satisfy $\gamma(I)$ is $i_0 = 1$ and $i_1 = -1$.

Therefore, the stabilizing (k_i, k_d) values corresponding to $k_p = 0.1$ must satisfy the string of the inequalities given by (30).

$$\begin{aligned} k_i &> 0 \\ k_i &> 1.2 \times 10^8 k_d - 446 \end{aligned} \tag{30}$$

The admissible set of values of (k_i, k_d) for which (30) is satisfied can be solved by linear programming. We can sweep over the entire range of k_p and find the (k_i, k_d) values.

4 Robust Stabilization of Interval Plant

The system parameters may have uncertainty which could lead to instability too. So, we proposed robust control to stabilize the interval plant. Kharitonov theorem is an extension of the Routh stability criterion to interval polynomials. An interval polynomial is a polynomial where each coefficient can vary in a prescribed interval. Consider the plant in (3) with uncertainty in its coefficients as given in (31).

$$G(s) = \frac{N(s,q)}{D(s,q)} = \frac{\sum_{i=0}^{m}[\underline{b_i}, \overline{b_i}]s^i}{\sum_{i=0}^{n}[\underline{a_i}, \overline{a_i}]s^i} = \frac{b_0}{a_2 s^2 + a_1 s + a_0} \tag{31}$$

where $b_0 \in \left[\underline{b_0}, \overline{b_0}\right]$, $a_1 \in [\underline{a_1}, \overline{a_1}]$, $a_0 \in \left[\underline{a_0}, \overline{a_0}\right]$, represent lower and upper bounds for parameters of both the numerator and denominator.

4.1 Kharitonov Theorem

A sufficient and necessary condition for stability of an interval plant is that the four polynomials given by (32) are stabilized hence they are Hurwitz:

$$\begin{aligned} K^1(s) &= \overline{a_0} + \overline{a_1}s + \underline{a_2}s^2 = 0 \\ K^2(s) &= \underline{a_0} + \underline{a_1}s + \overline{a_2}s^2 = 0 \\ K^3(s) &= \underline{a_0} + \overline{a_1}s + \overline{a_2}s^2 = 0 \\ K^4(s) &= \overline{a_0} + \underline{a_1}s + \underline{a_2}s^2 = 0 \end{aligned} \tag{32}$$

The proposed PID controller is used to stabilize the interval plant and its transfer function as mentioned in (7), so that the closed-loop characteristic polynomial $\delta\left(s, k_p, k_i, k_d\right)$ is Hurwitz. Let $N^i(s)$ and $D^j(s)$, i and $j = 1, 2, 3, 4$ are the Kharitonov polynomial of $N(s)$ and $D(s)$, respectively. Let $NS^i(s)$, $i = 1, 2, 3, 4$ be the four Kharitonov segments of $N(s)$ which make a convex combination where $\lambda \in [0, 1]$, are given in (33).

$$NS^1(s, \lambda) = \lambda N^1(s) + (1 - \lambda)N^2(s)$$

$$NS^2(s,\lambda) = \lambda N^1(s) + (1-\lambda)N^3(s)$$
$$NS^3(s,\lambda) = \lambda N^2(s) + (1-\lambda)N^4(s)$$
$$NS^4(s,\lambda) = \lambda N^3(s) + (1-\lambda)N^4(s) \quad (33)$$

By taking all combinations of the $NS^i(s,\lambda)$ and $D^j(s)$ for i and j = 1, 2, 3, 4, the family of 16 Kharitonov-segment plants, $G_S(s)$, are given by (34):

$$G_S(s) = G_{ij}(s,\lambda) = \frac{NS^i(s,\lambda)}{D^j(s)}, i = 1,2,3,4\ j = 1,2,3,4 \quad (34)$$

Then, the family of closed-loop characteristic polynomial for each segment plant $G_{ij}(s,\lambda)$ is denoted by (35):

$$\delta(s,k_p,k_i,k_d,\lambda) = sD^j(s) + (k_i + k_p s + k_d s^2)NS^i(s,\lambda) \quad (35)$$

The whole $G_S(s)$ family is stabilized by the proposed PID controller. We find k_p for every $G_{ij}(s,\lambda)$ with $\lambda \in [0,1]$, then find intersection and take a fixed value for k_p we can determine (k_i, k_d) set.

For our system $G(s)$ given in (31), the lower and upper bounds of parameters have been chosen based on the maximum capability of PID controller that could stabilize the system, for instance, larger power or inductance and lower capacitance than our specified bounds could lead to instability of the system and the PID will not be able to stabilize the system. The uncertain system parameters are:

$$40 < V_s < 60\,\text{V}, 23 < V_o < 27\,\text{V}, 50 < L < 200\,\mu\text{H},$$
$$350 < C < 600\,\mu\text{F}, 0.03 < r_L < 0.07\,\Omega, 135 < P < 1100\,\text{w}$$

Substitute in (31) to get the lower and upper bounds of coefficients as follows:

$$b_0 \in \left[3\times10^8, 3.4\times10^9\right], a_1 \in \left[7.34\times10^3, 1.12\times10^3\right], a_0 \in \left[2.2\times10^6, 5.7\times10^7\right]$$

So, the Kharitonov polynomials related to $N(s)$ and $D(s)$ are:

$$N^1(s) = 3.0\times10^8\ \ D^1(s = \left[17.34\times10^3 \quad 2.18\times10^6\right]$$
$$N^2(s) = 3.4\times10^9\ \ D^2(s) = \left[11.12\times10^3 \quad 5.7\times10^7\right]$$
$$N^3(s) = 3.4\times10^9\ \ D^3(s) = \left[17.34\times10^3 \quad 5.7\times10^7\right]$$
$$N^4(s) = 3.0\times10^8\ \ D^4(s = \left[11.12\times10^3 \quad 2.18\times10^6\right]$$

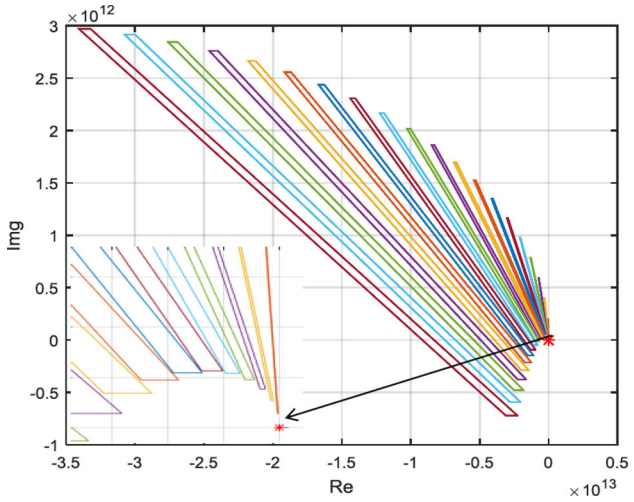

Fig. 6 Stability test of interval plants for $0 < \omega < 10^3$ rad/s

Solving for the first Kharitonov segment $G_{13}(s,\lambda)$ as an example given by (36)

$$G_{13}(s,\lambda) = \frac{NS^1(s,\lambda)}{D^3(s)} = \frac{\lambda N^1(s) + (1-\lambda)N^2(s)}{D^3(s)} = \frac{\lambda N^1(s) + (1-\lambda)N^2(s)}{s^2 7.34\times10^3 s + 5.7\times10^7} \quad (36)$$

We find k_p for every segment and for $\lambda \in [0,1]$ to be as given by (37)

$$k_p = \cap_{i=1.2.3.4,\, j=1.2.3.4} G_{ij}(s,\lambda) \quad (37)$$

Resulted in $k_p \in (0.008, \infty)$, Take a fixed value for k_p and solve the eight plants of $G_{ij}(s,\lambda)$ to find (k_i, k_d) stabilizing set using HB theorem.

5 Robust Stability

To inspect the robust stability of closed-loop characteristic polynomial given by (21), we applied zero exclusion condition (ZEC).

Assuming that $P = \{p(.,q) : q \in Q\}$ is an interval polynomial with invariant degree and has at least one stable member, then based on ZEC, P is robustly stable if origin of complex plane, i.e., Z = (0, 0), is excluded from the vertex plants for all $\omega \geq 0$, $0 \notin p(j\omega, Q)$ as shown in Fig. 6 between real (Re) and imaginary (Img).

We could also check stability of the uncertain system with the designed controller using root locus. We found that all the system poles are in the left half plane which means the same controller can stabilize the multi-model plant with parameter uncertainties as shown in Fig. 7

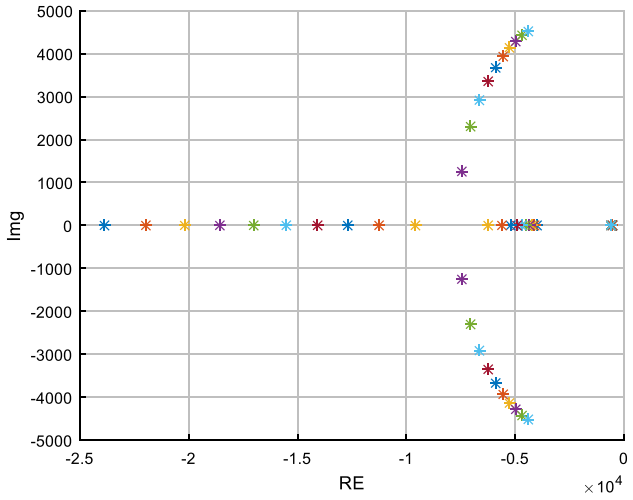

Fig. 7 Root locus of multi-model plant due to parameters uncertainties

6 Simulation Results

Based on Matlab–Simulink (R2015 a) software package and applying the proposed PID controller whose parameters are $k_p = 0.1, k_i = 20$, and $k_d = 10 \times 10^{-5}$ to the switched nonlinear model for two cases, normal case and uncertain case;

6.1 Normal Case

Assuming that the power of the CPL is changing as shown in Fig. 8a, and the system input (V_{ref}) is set at 24v, the system output, V_o, is shown in Fig. 8b. It is clear that the system is stable with variable CPL power. Moreover, although the load power increased abruptly from 500 to 800 W at time of 0.05 s, and increased again from 800 to 1100 W at 0.12 s and suddenly decreased from 1100 to 750 W at 0.16 s, the output tracked the reference voltage successfully with spikes at the points of power changes. Also there are some accepted ripples around the reference voltage as zoomed in the interval from 0.078 to 0.088 s shown in Fig. 8b.

The tracking error, which is the difference between the reference voltage (V_{ref}) and the output voltage (V_o), is shown in Fig. 9. From that figure, we observe that the PID controller succeeded to track V_{ref} with certain tolerance within $\pm 0.2\%$ with overshoot that doesn't exceed 1 V in transient state.

6.2 Uncertain Case

In order to validate the proposed algorithm with uncertainties, we compared the obtained simulation results using proposed PID controller ($V_{\text{outputPID}}$) with those obtained by relay control ($V_{\text{output relay}}$) given by Rafiezadeh (Grino and Rafiezadeh 2019). At the same power consumption of the CPL shown in Fig. 10a and the system inductance is increased from its

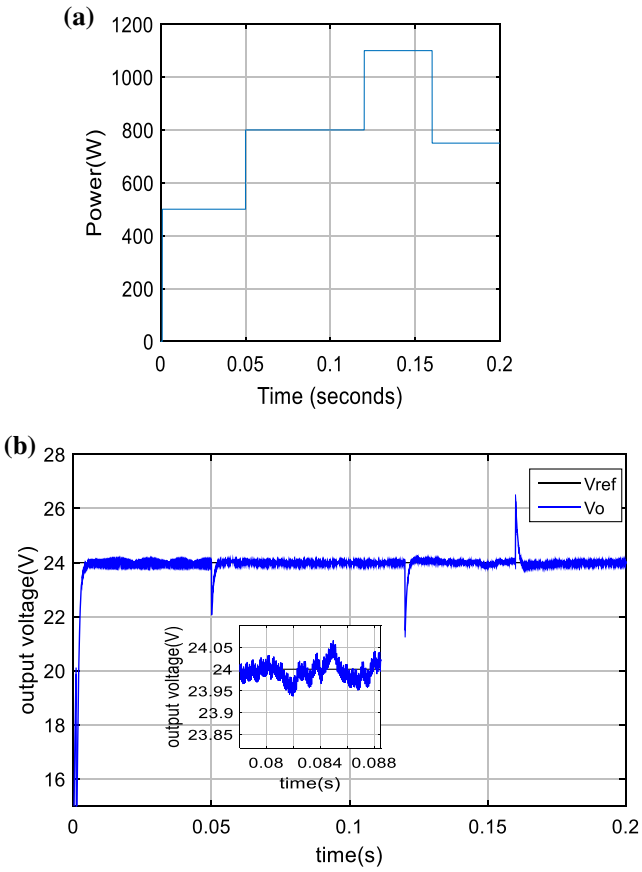

Fig. 8 **a** The power drawn by CPL. **b** The output voltage on capacitor

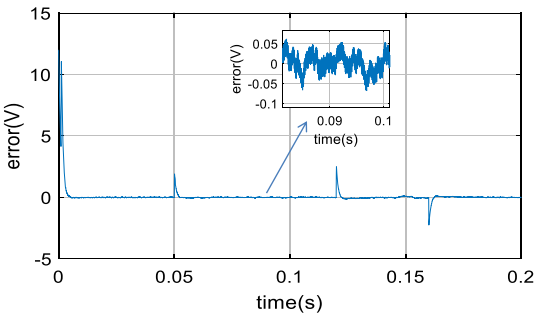

Fig. 9 Tracking error between the desired reference voltage and output voltage

nominal value (100 μH) to 150 μH and the capacitance is decreased from its nominal value (470 μF) to 350 μF, the comparison revealed that, our algorithm of the PID controller succeeded to stabilize the system and track the reference value (V_{ref}) as shown in Fig. 10b, but the relay method of (Grino and Rafiezadeh 2019) couldn't.

To examine the robustness of the proposed PID controller, the converter supply voltage V_s is decreased from 48 to 40 V at time 0.05 s then increased from 40 to 60 V at time 0.1 s as a disturbance in input voltage as shown by the red line in Fig. 11. It is clear that the output voltage with the pro-

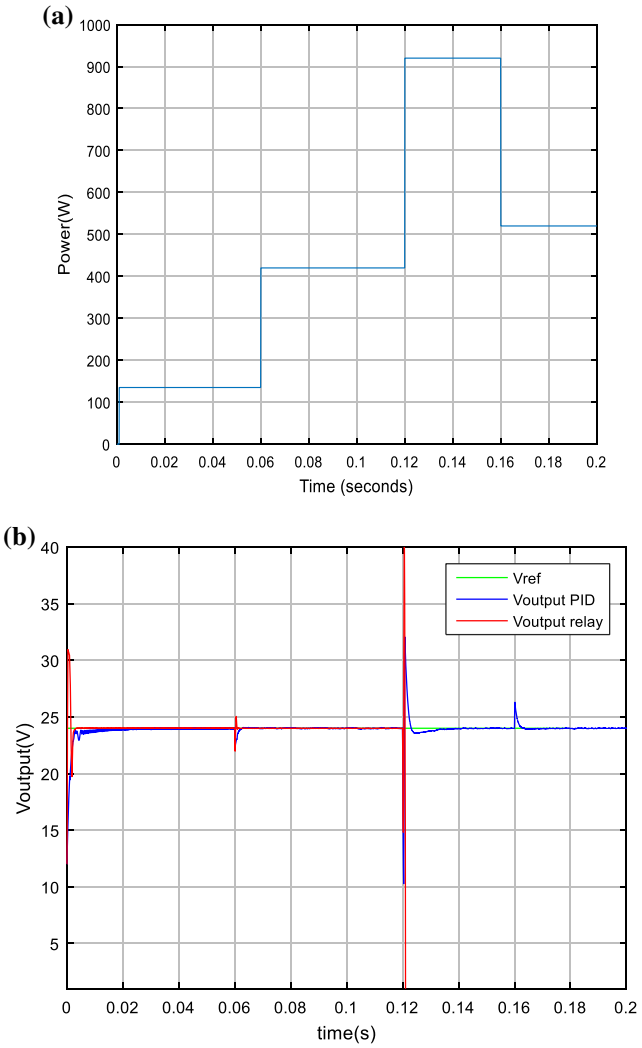

Fig. 10 **a** CPL power variation. **b** Output voltage with CPL variation

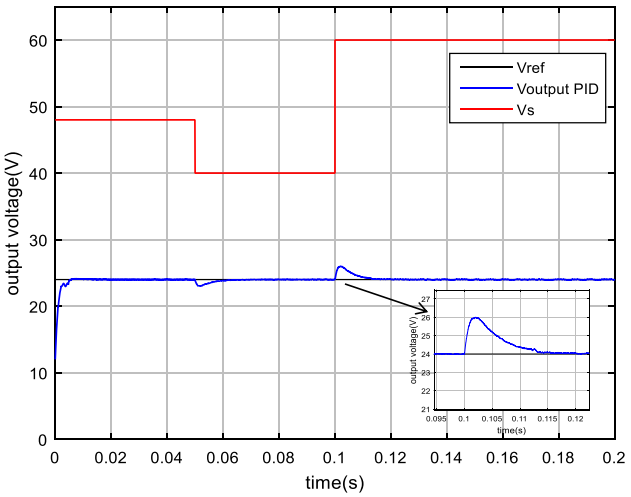

Fig. 11 Output voltage with source voltage variation

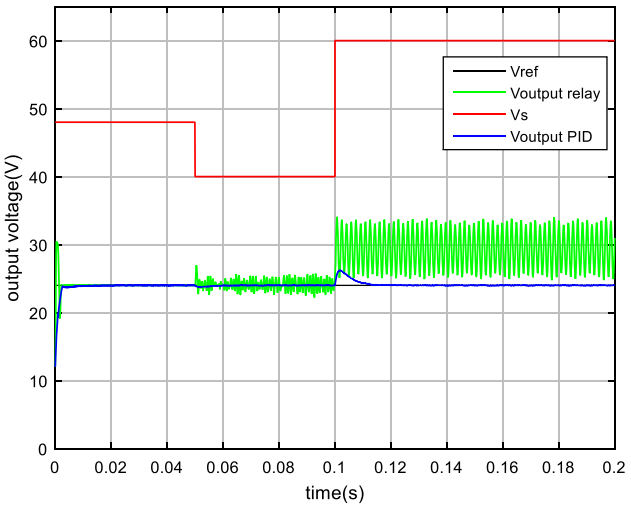

Fig. 12 Output voltage of PID and relay controller due to control signal disturbance

posed PID controller (blue line) is succeeded to track the reference voltage (V_{ref}). Moreover, when the supply voltage decreased, the output voltage is dropped by 1 V and returned to its reference value within time period of 10 ms. Furthermore, when the supply voltage is increased, the controller succeeded to track the reference voltage with overshoot of 2 V. This overshoot is disappeared within a time period of 10 ms too. The period when the supply voltage increased is zoomed into identify the overshoot occurred at that period of disturbance.

For the uncertain system parameters (L, C), a control signal disturbance could also added due to sensor noise at 0.05 s to both the proposed PID controller and the Relay controller given in Grino and Rafiezadeh (2019). The proposed PID was able to track the reference signal; however the relay controller output voltage had oscillation and it couldn't track the reference voltage, when the supply voltage is suddenly increased, as shown in Fig. 12. Comparison between the proposed method and Rafiezadeh's method in Grino and Rafiezadeh (2019)is given in Table 1.

Table 1 Comparison between the results of the proposed method with the results of Grino and Rafiezadeh (2019)

Comparison	Method in Grino and Rafiezadeh (2019)	Proposed method
Parameter uncertainty	Unstable	Stable
Control signal disturbance	Unstable	Stable
Maximum overshoot	1.8v	2v
Settling time	1 ms	10 ms

7 Conclusion

This paper presents a simple and robust method to control buck converter feeing constant power load (CPL). We used Hermite Biehler theorem and its generalization to find all the possible stabilizing sets. The multi-model plant enabled the PID controller to stabilize the system at different CPL operating points with parameter uncertainties. So the drawback of small signal stability methods were handled as the system is linearized around all the possible operating points using our proposed method. To assure robust stability, we applied zero exclusion condition to test it. The simulation results PID controller succeeded to track the reference voltage with small accepted tolerance. We validated the proposed algorithm by comparing it with previous research work and showed superior advantage. The proposed method has limitation in large gain values that lead to controller saturation or instability; so small gain values are selected. As a future work, we will focus on increasing stability region of the proposed controller and introduce a method for parameters tuning for a desired performance.

References

Ahmadi, R. (2013). *Dynamic modeling, stability analysis, and controller design*. Missouri University of Science and Technology, Doctoral dissertation 2013.

Dong, M., Liu, Z., Wang, S., Zhu, Q., Su, M., & Li, Y. (2017). Design criteria for parallel connected-buck converters in DC microgrid loaded by CPLs. In *Future Energy Electronics Conference and ECCE Asia (IFEEC 2017 - ECCE Asia)*, Kaohsiung, Taiwan.

Dragičević, T., Xiaonan, L., & Vasquez, J. C. (2016). DC microgrids—-Part I: A review of control strategies and stabilization techniques. *IEEE Transactions on Power Electronics, 31*(7), 4876–4891.

Emadi, A., & Ehsani, M. (2000). Negative impedance stabilizing controls for PWM DC–DC converters using feedback linearization techniques. In *Collection of Technical Papers. 35th Intersociety Energy Conversion Engineering Conference and Exhibit (IECEC)*, Las Vegas, NV, USA, USA.

Emadi, A., Khaligh, A., Rivetta, C. H., & Williamson, G. A. (2006). Constant power loads and negative impedance instability in automotive systems: definition, modeling, stability, and control of power electronic converters and motor drives. *IEEE Transactions on Vehicular Technology, 55*(4), 1112–1125.

Gavagsaz-Ghoachani, R., Martin, J. P., Pierfederici, S., Nahid-Mobarakeh, B., Molinas, M., & Zadeh, M. K. (2015). Discrete-time modelling, stability analysis, and active stabilization of DC distribution systems with multiple constant power loads. In *IEEE Applied Power Electronics Conference and Exposition (APEC)*, Charlotte, NC, USA.

Grino, R., & Rafiezadeh, R. (2019). A relay controller with parallel feed-forward compensation for a buck converter feeding constant power loads. In *2019 24th IEEE international conference on Emerging Technologies and Factory Automation (ETFA)*, Spain.

Herrera, L., Zhang, W., & Wang, J. (2017). Stability analysis and controller design of DC microgrids with constant power loads. *IEEE Transactions on Smart Grid, 8*(2), 881–888.

Ho, M., Bhattacharyya, S. P., & Datta, A. (2000). *Structure and synthesis of PID controllers*. London: Springer.

Hu, J., Zhao, Z., & Shao, X. (2019). Stabilisation strategy based on feedback linearisation for DC microgrid with multi-converter. *The Journal of Engineering, 2019*(16), 1802–1806.

Kwasinski, A., & Krein, P. T. (2007). Passivity-based control of buck converters with constant-power loads. In *IEEE Power Electronics Specialists Conference*, Orlando, FL, USA.

Lindahl, P. A., Banerjee, A., Leeb, S. B., & Gutierrez, M. (2019). An energy buffer for controllable input impedance of constant power loads. *IEEE Transactions on Industry Applications, 55*(3), 2910–2921.

Lonkar, M., & Ponnaluri, S. (2015). An overview of DC microgrid operation and control. In *IREC2015 The Sixth International Renewable Energy Congress*, pp. 1–6.

Lu, X., Vasquez, J. C., & Guerrero-Dragičević, J. M. (2016). DC microgrids—Part II: A review of power architectures, applications, and standardization issues. *IEEE Transactions on Power Electronics, 31*(5), 3528–3549.

Nahid-Mobarakeh, B., Pierfederici, S., Meibody-Tabar, F., & Awan, A. B. (2009). *Nonlinear stabilization of a DC-bus supplying a constant power load*, Houston, TX, USA, pp. 1–8.

Nahid-Mobarakeh, B., Pierfederici, S., & Zahedi, B. (2016). A robust active stabilization technique for DC microgrids. In *Power Electronics and Motion Control Conference (PEMC)*, Varna, Bulgaria.

Onwuchekwa, C. N., & Kwasinski, A. (2010). Analysis of boundary control for buck converters with instantaneous constant-power loads. *IEEE Transactions on Power Electronics, 25*(8), 2018–2032.

Perez, R., & Hossain, E. (2017). Development of Lyapunov redesign controller for microgrids with constant power loads. *Renewable Energy Focus, Science Direct, 19–20,* 49–62.

Rahimi, A. M., & Emadi, A. (2009). Active damping in DC/DC power electronic converters: A novel method to overcome the problems of constant power loads. *IEEE Transactions on Industrial Electronics, 56*(5), 1428–1439.

Rivetta, C. H., Emadi, A., Williamson, G. A., Jayabalan, R., & Fahimi, B. (2006). Analysis and control of a buck DC-DC converter operating with constant power load in sea and undersea vehicles. *IEEE Transactions on Industry Applications, 42*(2), 559–572.

Rivetta, C., & Williamson, G. A. (2003). Large-signal analysis of a DC–DC buck power converter operating with constant power load. In *The 29th annual conference of the IEEE Industrial Electronics Society, IECON'03* (Vol. 1, pp. 732–737), Roanoke, VA, USA.

Srinivasan, M. (2017). *Hierarchical control of DC microgrids with constant power loads*. University of Texas, Doctoral dissertation 2017.

Tahim, A. P. N. (2011). Control of interconnected power electronic converters in DC distribution systems. In *Power Electronics Conference (COBEP), Brazilian IEEE*, pp. 269–274.

Vafamand, N., Khooban, M. H., Dragičević, T., Blaabjerg, F., & Mardani, M. M. (2019). Design of quadratic D-stable fuzzy controller for DC microgrids with multiple CPLs. *IEEE Transactions on Industrial Electronics, 66*(6), 4805–4812.

Vu, T. (2016). *Distributed robust adaptive droop control for DC microgrids*. Florida State University, Florida, Doctoral dissertation 2016.

Williamson, G. A., Emadi, A., & Rahimi, A. M. (2010). Loop-cancellation technique a novel nonlinear feedback to overcome the destabilizing effect of constant-power loads. *IEEE Transactions on Vehicular Technology, 59*(2), 650–661.

Williamson, G. A., & Rivetta, C. (2004). *Global behaviour analysis of a DC–DC boost power converter operating with constant power load* (Vol. 5, p. 956), Vancouver, BC, Canada.

Ye, Q. (2017). *Small signal instability assessment and mitigation in power electronics based power systems*. Department of Electrical and Computer Engineering, Department of Electrical and Computer Engineering, Florida State University, Doctoral dissertation 2017.

Zhang, W., Rizzoni, G., & Liu, J. (2018). Robust stability analysis of DC microgrids with constant power loads. *IEEE Transactions on Power Systems, 33*(1), 748–753.

Zhao, Y., Qiao, W., & Ha, D. (2014). A sliding-mode duty-ratio controller for DC/DC buck converters with constant power loads. *IEEE Transactions on Industry Applications, 50*(2), 1448–1458.